City Research Online

City, University of London Institutional Repository

Determination of the hydrodynamic performance of marine propellers using fibre Bragg gratings

Matthias Fabian*[a], Bruno Rente[a], Saeed Javdani[b], Sara Uceda[b], Ian Godfrey[b], Ben Young[c], John Carlton[a], Tong Sun[a], Kenneth T.V. Grattan[a],

[a]City, University of London, 10 Northampton Square, London, EC1V 0HB, UK; [b]Teignbridge Propellers International Ltd., Great Western Way, Forde Road, Newton Abbot, TQ12 4AW, UK; [c]University of Queensland, Brisbane, QLD 4072, Australia

ABSTRACT

A critical aspect in the design of marine propellers is their hydrodynamic performance which, when evaluated experimentally, requires a number of parameters to be monitored at the same time, i.e. the thrust and torque a propeller generates as well as the propeller shaft and vessel speed. In this investigation, three of those parameters are measured using Fibre Bragg Grating-based sensors, thus allowing for computationally derived performance values to be verified. For that purpose, open water tests were carried out where an instrumented propeller shaft was installed into a research vessel and measurements taken, evaluated and the results compared favorably with advanced computer-based simulations.

Keywords: Optical fibre sensors, fibre Bragg gratings, torque, thrust, marine propeller, hydrodynamic performance

1. INTRODUCTION

The hydrodynamic performance of marine propellers comprises of a set of coefficients (as discussed in Section 2) that are traditionally determined from 'model-based' experiments, i.e. using small-scale propellers running at high speed and having small diameters, of the order of 200-300 mm. However, it is essential to understand the propeller performance characteristics both at lower speeds and larger diameters (up to 11 meters) by extrapolating from such model scale results. The reason for that is that while the flow is laminar over significant parts of a model-scale propeller blade, this is not the case for full-scale propellers where the flow is primarily turbulent over the blade surface[1].

In order to quantify the effect of scale on propeller performance, a number of analytical tools have been developed in the early to mid-1980s but a certain degree of empiricism[1] is still necessary. With the recent advancement in Computational Fluid Dynamic (CFD) capabilities, the marine industry largely shifted to the use of such CFD analysis to predict propeller performance at full-scale. However, it is essential to experimentally validate those simulations against the results from full-scale trials.

While torque meters are widely available for a whole range of shaft diameters and dynamic ranges, monitoring thrust still poses a challenging task. Conventional thrust sensors are either limited for propeller shafts larger than 200 mm in diameter[2] or are based on strain gauges[3] which tend to fail in the oily environment they are operating. Optical fibre-based sensors, however, are well suited to operate in such environments due to their chemical inertness and multiplexing capability which minimizes wiring efforts (as opposed to strain gauges) which is essential on rotating structures.

Teignbridge Propellers International Ltd. have built a catamaran research vessel equipped with a podded propulsion system submerged below its hull to minimize the wake effects on the propeller advance velocity (speed in water). Testing propellers of up to 1.2 meters diameter on the research vessel enables the propeller performance to be monitored in an open water environment which is similar to the operating condition of a full-scale propeller. In addition, the flow over the surface of propeller blades is fully turbulent unlike the transitional flow in typical, smaller model-scale propellers.

To study this, a propeller shaft of the propulsion system of the research vessel was instrumented with a number of FBGs to monitor the torque and thrust generated by the propeller as well as the shaft's rotational speed. The experimental results obtained from the sea trials are compared with the outcomes of CFD simulations which currently are used to validate the predicted propeller performance.

2. SENSOR DESIGN AND EXPERIMENTAL SETUP

The working principle of the FBG-based sensors used as the basis of this monitoring system has been widely reported, e.g.

in the work of Rao[4], and will therefore not be repeated here. In order to create the sensors used in this study, five FBGs of 5 mm in length were inscribed into germanium-doped photosensitive fibre (Fiber Core SM1500(4.2/125)) using an excimer laser (ATL 300 SI, 245nm) and the phase mask technique[1].

The sensor layout for both torque and thrust monitoring is shown in Figure 1. Two FBGs were attached to the propeller shaft at an angle of ±45° with respect to the spinning axis. In this configuration, the distance (in nm) between the two FBG reflection peak wavelengths (differential mode wavelength, DMW) was used as a measure for torque, whereas their mid-point (common mode wavelength, CMW) was used as an indicator for the temperature at that location[4,5]. In this investigation, however, the mid-point is used as a measure for thrust and a third FBG, which is strain relieved, is added for temperature compensation purposes. The sensing fibre was bonded to the shaft using a two-part epoxy adhesive that can withstand the oily environment that was present. Another such layout was attached to the opposite side of the shaft (without a temperature FBG) to compensate shaft bending (hence the total of 5 FBGs that were used).
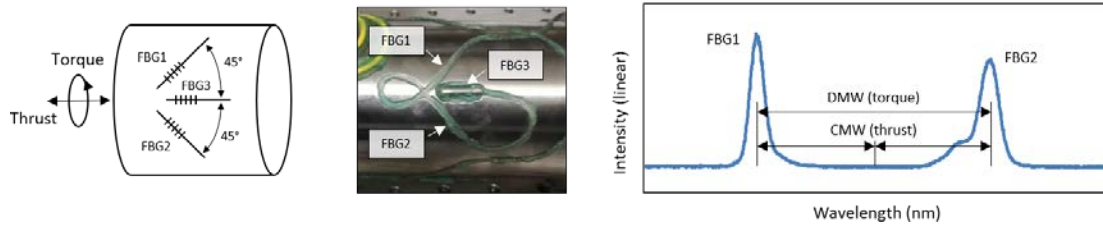

Figure 1. Sensor layout (left and centre) and sensing principle (right).

The sensors were calibrated for torque and thrust using a purpose-made test rig (Figure 2) where loads are applied to the shaft using a winch and a system of pulleys which can be arranged to apply torque only, thrust only, or both simultaneously. The actual values for torque and thrust generated by different winch loads were calculated from strain gauge data[3] which were attached next to the FBGs (those strain gauges were removed after the calibration was carried out). The temperature calibration was carried out in an oven where the FBG peak wavelength shifts of the individual sensors were recorded, creating a calibration of the system for a range of different temperatures.
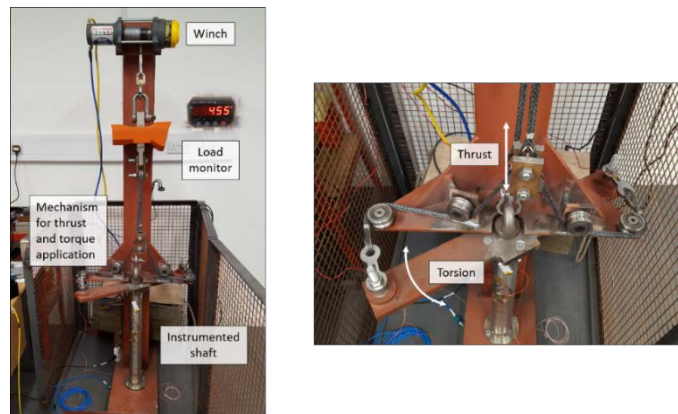

Figure 2. Calibration rig using a winch and a set of pulleys to apply torque and thrust to the instrumented shaft.

The calibration results are shown in Figure 3 for both torque (up to 2400 Nm) and thrust (up to 7.5 kN). It is clear from Figure 3 that, for torque only, the cross sensitivity is less than 1% whereas for thrust only the cross sensitivity is almost10%. This is most likely caused by the angles of the sensor layout not being exactly the designed value of ±45° (this being hard to achieve) but which is taken into account analytically as explained below. The calibration parameters used are summarized in Table 1.

In order to derive torque (Q) and thrust (T) from the sensor information, i.e. from CMW and DMW, equations 1-3 were used. Equation 1 describes the relationship between the sensor data and Q/T by use of a calibration parameter matrix (which takes into account the cross sensitivities addressed above). Equation 2 is a simplified version of equation 1 where the vectors/matrix are represented by symbols. Equation 3 is a rearranged version of equation 2 yielding torque and thrust from the inverted calibration parameter matrix and the wavelength information coming from the FBGs. Before the CMW and DMW could be calculated, the temperature induced peak wavelength shifts of each FBG were individually
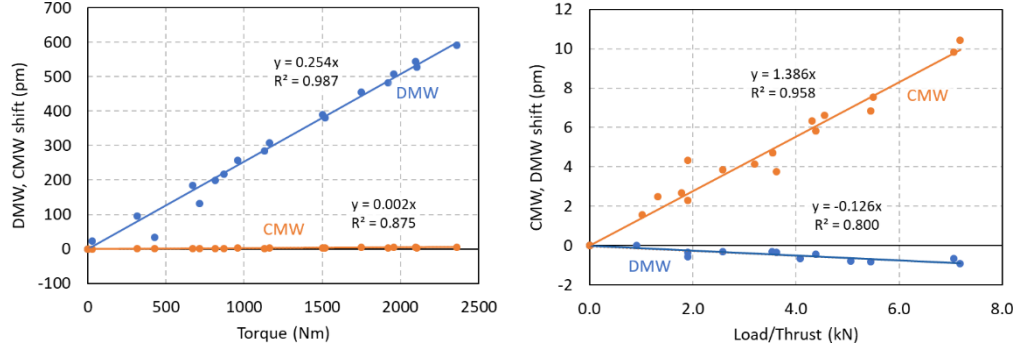
compensated for.

Figure 3. Calibration results for torque (left) and thrust (right) obtained in the laboratory for the sensor system designed.

Table 1. Calibration parameters for torque and thrust with regard to the common and differential mode wavelengths.

Parameter	Torque sensitivity (pm/Nm)	Thrust sensitivity (pm/kN)
DMW	0.254 (Q_{DMW})	-0.126 (T_{DMW})
CMW	0.002 (Q_{CMW})	1.386 (T_{CMW})

$$\begin{bmatrix} DMW \\ CMW \end{bmatrix} = \begin{bmatrix} Q_{DMW} & T_{DMW} \\ Q_{CMW} & T_{CMW} \end{bmatrix} \begin{bmatrix} Q \\ T \end{bmatrix} \tag{1}$$

$$\lambda = C \cdot TQ \tag{2}$$

$$TQ = C^{-1} \cdot \lambda \tag{3}$$

The propeller performance is typically described by a set of non-dimensional coefficients defined as:

$$K_T = \frac{T}{\rho n^2 D^4} \qquad K_Q = \frac{Q}{\rho n^2 D^5} \qquad J = \frac{v_a}{nD} \qquad \eta = \frac{T v_a}{2\pi n Q} \tag{4}$$

where, K_T and K_Q are the thrust and torque coefficients respectively, J the advance ratio, η the hydrodynamic efficiency, ρ the density of water, n the propeller rotational speed, D the propeller diameter and v_a the advance speed of the vessel (speed in water). All four coefficients are crucial in propeller theory, contributing to the hydrodynamic performance of a propeller.

3. RESULTS AND DISCUSSION

After the successful calibration was undertaken, the instrumented shaft was installed on the research vessel and a 16-minute open water test run (a two way run, 180 deg apart, with each leg taking approximately 8 minutes) was carried out at different speeds to evaluate the propeller performance. For that purpose, the sensing fibre was connected to a sensing interrogator unit (Micron Optics SM130) through a fibre-optic rotary joint which was mounted at the rear end of the shaft.

The tested propeller under test had a diameter of 1.2 meter and is primarily designed for a handy-size bulk carrier vessel which at full-scale has a propeller dimeter of approximately 5.25m. The vessel speed through water was monitored by two Doppler Velocity Logs (DVLs) while the propeller shaft rotational speed, thrust, torque and consequently the hydrodynamic efficiency were derived from the FBG sensor data (the shaft speed in rotations per minute was obtained from the AC part of one of the FBGs through FFT analysis[7]).

The propeller performance in terms of its thrust and torque coefficients, as well as its hydrodynamic efficiency at varying advance velocities are shown in Figure 4 where the experimental results (dots) are compared to those predicted by the CFD simulations. It can be seen that there is a good correlation between the results within the range of advance velocities were the propeller was tested. The relative difference between the measured hydrodynamic efficiency of the propeller and those predicted by the CFD simulations are given in Table 2 in an ascending order of the advance ratio.
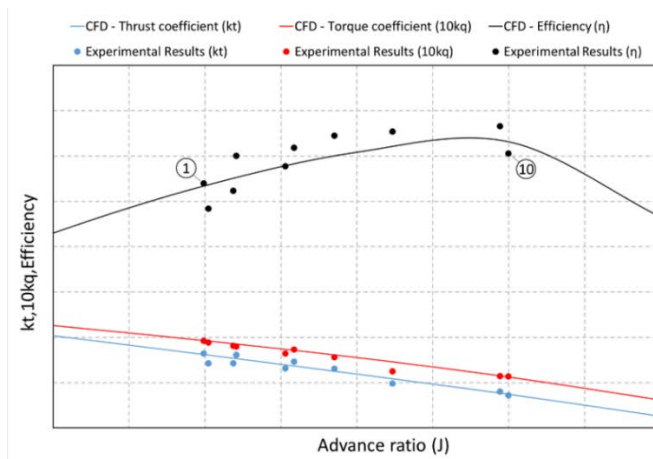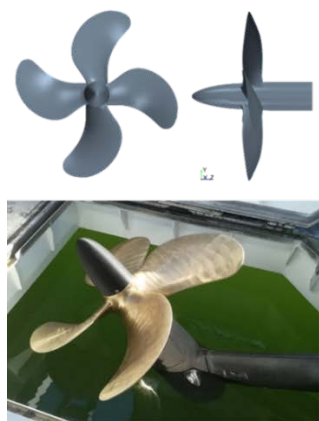
Figure 4. Hydrodynamic performance of an example propeller tested on the research vessel; Sea trial test results (dots) plotted against the predicted performance with CFD simulations (lines).

Table 2. Relative difference in thrust and torque coefficients and propeller hydrodynamic efficiency (ID No. 1 indicates the lowest advance ratio as shown in Figure 5)

Advance Ratio (J) ID No.	1	2	3	4	5	6	7	8	9	10
ΔKt (%)	0.94	-11.28	-7.48	5.15	-5.52	7.07	4.33	-9.32	6.10	-1.95
ΔKq (%)	-0.42	-1.85	-2.68	-3.23	-5.21	1.09	-2.62	-13.62	0.87	2.25
$\Delta\eta$ (%)	1.37	-9.60	-4.93	8.67	-0.33	5.92	7.13	4.98	5.19	-4.11

4. CONCLUSIONS

It was demonstrated that the performance of the sensor system developed and the test carried out that marine propellers can be reliably evaluated using Fibre Bragg Grating-based sensors by exploiting their capability of monitoring multiple parameters in a multiplexed sensing approach. Proof-of-principle test were carried out on a research vessel in open water and the obtained results closely matched those of obtained from the CFD analysis.

ACKNOWLEDGEMENTS

REFERENCES

[1] Carlton, J., [Marine Propeller and Propulsion] Oxford: Butterworth-Heinemann, 3rd Edition, 79-136 (2012).
[2] VAF Instruments, "TT-Sense, torque and thrust measurement," https://www.vaf.nl/products-solutions/overview/tt-sense-shaft-power-thrust-meter/.
[3] de Waal, R.J.O., Bekker, A. and Heyns, P.S., "Bi-polar full-scale measurements of operational loading on polar vessel shaft-lines," Proc. POAC'17, vol 1, 589-606 (2017).
[4] Rao, Y. J., "In-fibre Bragg grating sensors," Meas. Sci. Technol. 8(4), 355–375 (1997).
[5] Swart, P. L., Chtcherbakov A. A. and van Wyk A. J., "Dual Bragg grating sensor for concurrent torsion and temperature measurement," Meas. Sci. Technol. 17(5), 1057–1064 (2006).
[6] Wang, Y., Liang, L., Yuan, Y., Xu, G. and Liu F., "A two fibre bragg grating sensing system to monitor the torque of rotating shaft," Sensors 16 (1), 138 (2016).
[7] Fabian, M., Hind, D., Gerada, C., Sun, T. and Grattan, K.T.V., "Comprehensive monitoring of electrical machine parameters using an integrated fibre bragg grating -based sensor system," JLT 36(4), 1046-1051 (2018).